

Hyperfine spectroscopy using co-propagating pump-probe beams

Alok K. Singh, Sapam Ranjita Chanu, Dipankar Kaundilya and Vasant Natarajan*
Department of Physics, Indian Institute of Science, Bangalore 560 012, INDIA

We have shown earlier that hyperfine spectroscopy in a vapor cell using co-propagating pump-probe beams has many advantages over the usual technique of saturated-absorption spectroscopy using counter-propagating beams. The main advantages are the absence of crossover resonances, the appearance of the signal on a flat (Doppler-free) background, and the higher signal-to-noise ratio of the primary peaks. Interaction with non-zero-velocity atoms causes additional peaks, but only one of them appears within the primary spectrum. We first illustrate the advantages of this technique for high-resolution spectroscopy by studying the D_2 line of Rb. We then use an acousto-optic modulator (AOM) for frequency calibration to make precise hyperfine-interval measurements in the first excited $P_{3/2}$ state of $^{85,87}\text{Rb}$ and ^{133}Cs .

PACS numbers: 32.10.Fn, 42.62.Fi, 42.50.Gy

I. INTRODUCTION

High-resolution laser spectroscopy has been revolutionized in the last two decades with the advent of low-cost tunable diode lasers [1]. These diodes, when placed in an external cavity with optical feedback, have frequency uncertainty of about 1 MHz, which is small enough for hyperfine transitions in atoms to be resolved [2, 3]. Hyperfine spectroscopy, particularly in the low-lying electronic states of alkali-metal atoms, plays an important role in fine-tuning atomic wavefunctions used in theoretical calculations. This is because comparison between theoretical and experimental determinations of hyperfine structure provides a stringent test of atomic calculations in the vicinity of the nucleus [4]. In addition, hyperfine structure in these multielectron atoms is sensitive to core polarization and core correlation effects [5].

Many of the alkali-metal atoms have transitions to the first-excited state (so-called D lines) which are in the near infrared, and therefore accessible with diode lasers. They also have a high-enough vapor pressure near room temperature that the spectroscopy can be done in a vapor cell. The thermal motion of the atoms inside the cell causes *Doppler broadening*, which is typically 100 times larger than the natural width of the hyperfine transitions. The standard technique to overcome the first-order Doppler effect is to use a *counter-propagating* pump beam to saturate the transition for zero-velocity atoms, in what is called saturated-absorption spectroscopy (SAS) [6].

Most atoms also have several closely-spaced hyperfine levels within the Doppler profile. In these cases, it is well known that SAS also produces spurious crossover resonances in between each pair of hyperfine transitions. They occur because, for some non-zero-velocity group, the pump drives one transition while the probe drives the other. In earlier work [7], we have shown that the use of co-propagating pump and probe beams overcomes

the problem of crossover resonances. Closely-spaced levels that are not resolved in SAS can be resolved by this technique. Probe transmission in such multilevel atoms is caused by the phenomenon of electromagnetically induced transparency (EIT) [8, 9], and population depletion due to optical pumping. Furthermore, by scanning only the pump beam, the signal appears on a flat background without the underlying Doppler profile seen in SAS. This is advantageous for applications such as laser locking or laser frequency measurement.

In this work, we present a complete study of the spectra taken with the co-propagating technique in the D_2 line of the two isotopes of Rb. In particular, we show that the effect of non-zero velocity groups is to cause additional peaks. However, in contrast to SAS, only one of these spurious peaks appears within the spectrum, and the real peaks are unaffected. Interestingly, the spurious peak within the spectrum is almost negligible for transitions starting from the upper ground hyperfine level, but highly prominent for transitions starting from the lower level. Such differences between the two levels have also been seen in EIT, arising from the fact that the closed transition is $F \rightarrow (F+1)$ for the upper hyperfine set and $F \rightarrow (F-1)$ for the lower hyperfine set.

For a second set of experiments, we have used a single laser along with an acousto-optic modulator (AOM) to produce the pump-probe beams with a precisely-controlled frequency offset. We then obtain the entire spectrum by scanning the frequency of the AOM. The scan axis is guaranteed to be linear because it is determined by the frequency of the rf oscillator driving the AOM. A curve fit to the observed spectrum yields the hyperfine interval. The measurements have an accuracy of 20 kHz, which is comparable to the accuracy of other techniques.

In recent work from our laboratory, we have reported high-accuracy values for the hyperfine constants in the D lines of all alkali atoms [10]. The hyperfine intervals in that work were obtained (with an accuracy of 6 kHz) by *locking* the AOM to the neighboring transition. One of the uncertainties when locking the AOM is whether the lock point is exactly at the center of the peak, since any

*Electronic address: vasant@physics.iisc.ernet.in;
 URL: www.physics.iisc.ernet.in/~vasant

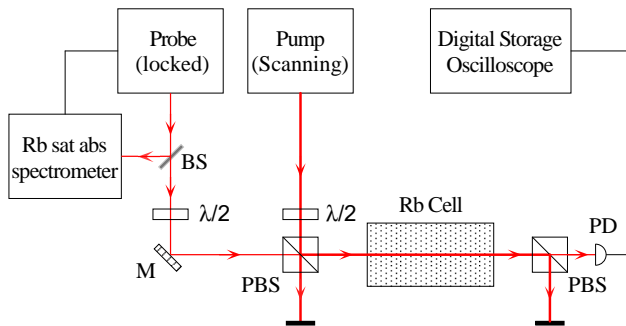


FIG. 1: Schematic of the experiment. Figure key: BS – beam-splitter, $\lambda/2$ – halfwave retardation plate, M – mirror, PBS – polarizing beamsplitter cube, PD – photodiode.

shift would cause a systematic error in the measurement. Though we had done experiments to verify that this error was less than 2 kHz, we wanted to repeat the measurements with another technique that was not at all susceptible to errors arising from lock-point uncertainty. As we will see below, the co-propagating technique achieves precisely this. In addition, by measuring the entire spectrum and looking at the symmetry of the line shape, we can be sure that other sources of error are not significant. The current set of measurements in ^{85}Rb and ^{133}Cs , although having slightly smaller precision, are consistent with our earlier work.

II. SPECTROSCOPY ON THE D_2 LINE OF RUBIDIUM

The schematic for the first set of experiments is shown in Fig. 1. The pump and probe beams are derived from two home-built frequency-stabilized diode laser systems [3] operating on the 780 nm D_2 line of Rb. The linewidth of the lasers after stabilization is of the order of 1 MHz. The output beams are elliptical with $1/e^2$ size of 2×4 mm and powers of around $10 \mu\text{W}$ each. Part of the probe laser is sent into a Rb SAS cell and the laser is locked to a hyperfine transition using fm modulation spectroscopy. The pump laser is scanned around the same set of transitions. The beams are mixed in a polarizing beamsplitter cube (PBS) and *copropagate* through a room-temperature vapor cell (5 cm long) with orthogonal linear polarizations. Halfwave retardation plates in the path of each beam allow precise control of their powers. The probe beam is separated using a second PBS, and its transmitted signal is detected with a photodiode. The PBS's have extinction ratios of 1000 : 1, ensuring good purity of the detected signal.

A. Spectrum in ^{87}Rb , $F = 2 \rightarrow F' = 1, 2, 3$

As mentioned before, the main advantage of the co-propagating configuration is the absence of spurious

crossover resonances. This difference is seen clearly in Fig. 2. In (a), we show the usual saturated-absorption spectrum for the $F = 2 \rightarrow F' = 1, 2, 3$ transitions in ^{87}Rb . The spectrum is Doppler corrected, which is necessary because probe absorption through a vapor cell will show a broad Doppler profile when the probe addresses a velocity group different from that resonant with the pump. When the pump and probe are resonant with the same velocity class, we get transmission peaks. As expected, there are three hyperfine peaks and three crossovers. The crossovers are more prominent than the actual peaks because two velocity classes contribute to each crossover resonance, compared to one (zero-velocity) class for each hyperfine peak. Probe transparency is primarily caused by two effects: (i) saturation of absorption caused by the strong pump beam, and (ii) optical pumping into the $F = 1$ ground hyperfine level for open transitions (i.e. those involving the $F' = 1$ and 2 excited levels). In addition, there will be population redistribution among the magnetic sublevels, which can cause increased absorption or transparency depending on the F values of the levels. The linewidth of the peaks in the figure is about 12 MHz, compared to the natural linewidth of 6 MHz. This increase is typical in SAS and arises due to a misalignment angle between the beams and power broadening.

Now let us consider the spectrum shown in (b) taken with the co-propagating configuration. The probe is locked to the $F = 2 \rightarrow 3$ transition and the pump is scanned across the set of $F = 2 \rightarrow F' = 1, 2, 3$ transitions. Since the probe is locked, its transmitted signal primarily corresponds to absorption by zero-velocity atoms (i.e. atoms moving perpendicular to the laser beam) making transitions to the $F' = 3$ level. The signal remains flat (or Doppler free) until the pump also comes into resonance with a transition for the same zero-velocity atoms. Thus there are three transmission peaks at the locations of the hyperfine transitions, with no crossover resonances in between. The hyperfine peaks are located at -423.600 MHz, -266.657 MHz, and 0 [10], all measured with respect to the frequency of the locked probe laser. The linewidth of the peaks is about 19 MHz, which is only 50% larger than the linewidth obtained in the saturated-absorption spectrum. The primary cause for the transparency peaks is the phenomenon of EIT in this V-type system. The pump laser causes an *AC Stark shift of the ground level* (creation of dressed states [11]) and hence reduces probe absorption at line center. In addition, there are effects of saturation and optical pumping, but these are less important than the EIT effects.

Since the experiments are done in a vapor cell with the full Maxwell-Boltzmann distribution of velocities, we have to consider that there will be two additional velocity classes that absorb from the locked probe: both moving in the same direction as the probe but with velocities such that one drives transitions to the $F' = 2$ level (266.657 MHz lower) and the second to the $F' = 1$

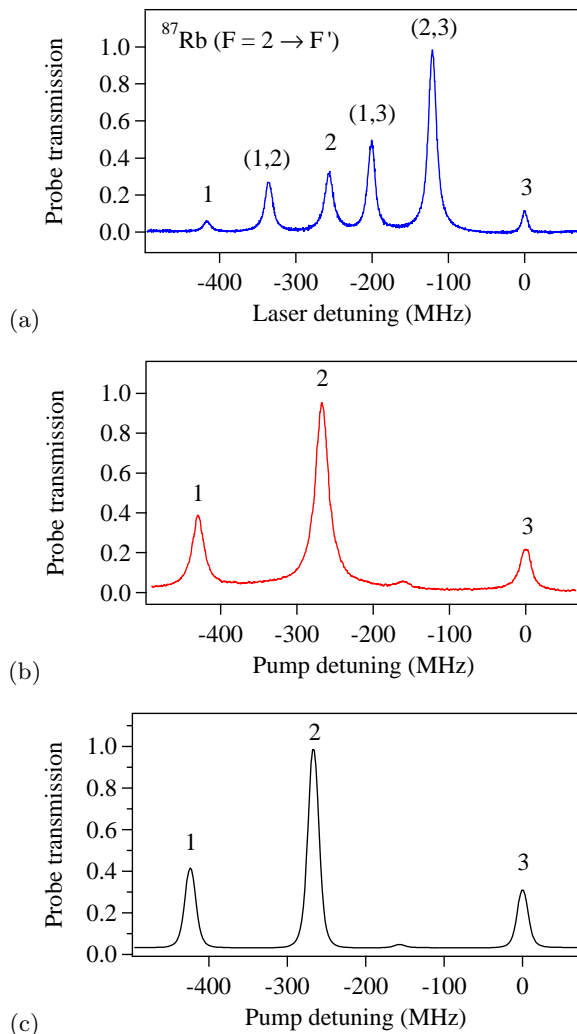


FIG. 2: (a) Doppler-subtracted saturated-absorption spectrum for $F = 2 \rightarrow F'$ transitions in ^{87}Rb . The hyperfine transitions are labelled with the value of F' , and the crossover resonances in between with the two values of F' . (b) Spectrum taken with co-propagating pump-probe beams, with probe locked to the $F = 2 \rightarrow 3$ transition and pump scanning. Note the absence of crossover resonances and the better signal for the hyperfine peaks. There is one additional peak at -157 MHz, as explained in the text. (c) Calculated spectrum taking into account the full thermal velocity distribution.

level (423.600 MHz lower). Each of these will cause three additional transparency peaks from the mechanisms discussed above. The first velocity class moves at 208 m/s and will cause peaks at -156.943 MHz, 0, and $+266.657$ MHz, i.e., a set of peaks shifted up by 266.657 MHz. The second velocity class moves at 330 m/s and will cause peaks at 0, 156.943 MHz, and $+423.600$ MHz, i.e., a set of peaks shifted up by 423.600 MHz. Thus there will be 7 peaks in all, with 3 real peaks and 4 spurious ones. However, only the peak at -156.943 MHz will appear within the spectrum, caused by the probe driving the $F = 2 \rightarrow F' = 2$ transition and the pump driving the

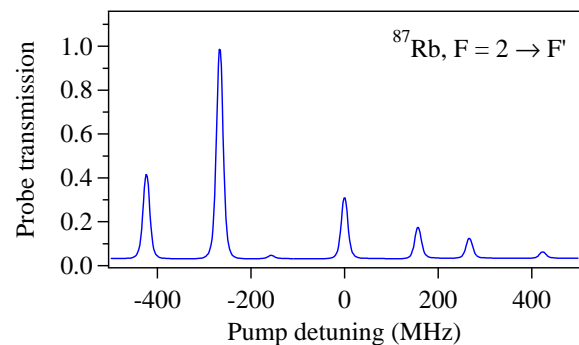


FIG. 3: Calculated spectrum extending on the other side of the locked probe peak. There are now 7 peaks, as explained in the text.

$F = 2 \rightarrow F' = 1$ transition. The other three spurious peaks will lie outside the spectrum to the right. This is indeed what is observed in Fig. 2(b): there is a small peak at -157 MHz within the spectrum.

The above explanation is borne out by the calculated spectrum shown in Fig. 2(c). Using a density-matrix formulation, we can calculate the absorption of a probe laser in a V-type system [9]. The calculation is done for multiple hyperfine levels with full thermal averaging. The only adjustable parameters are the relative amplitudes of the three EIT resonances. As seen from the figure, the calculation reproduces the locations of the peaks in the measured spectrum. The observed linewidth is slightly larger than the calculated one, but this could be because of a small misalignment angle between the beams, which is known to broaden the EIT resonance [12]. The calculation shows that there is only one spurious peak within the spectrum. However, if we extend the calculation up to $+500$ MHz, we see all the seven peaks mentioned in the previous paragraph. The extended calculation is shown in Fig. 3.

The advantages of this scheme are quite clear from Fig. 2(b). The spectrum appears on a flat background, obviating the need for Doppler subtraction as in the case of SAS. There are no crossover resonances, which often swamp the true peaks. And there is only one additional peak within the spectrum due to absorption by non-zero velocity atoms. In Fig. refcoprop, we show the effect of pump power on the peaks. As the power is varied from 0.33 to 1.66 times the probe power, the three main peaks remain quite prominent with good signal-to-noise ratio. The additional peak at -157 MHz increases in height, but not significantly. By comparison, a good saturated-absorption spectrum requires the pump-probe power ratio to be accurately controlled to a value of 3 : 1, with loss in signal at lower pump powers and power broadening at higher powers. In Fig. 4(b), we show a multipeak Lorentzian fit to the spectrum measured with a pump power of $15 \mu\text{W}$. The residuals show that the line shape of all the peaks is Lorentzian.

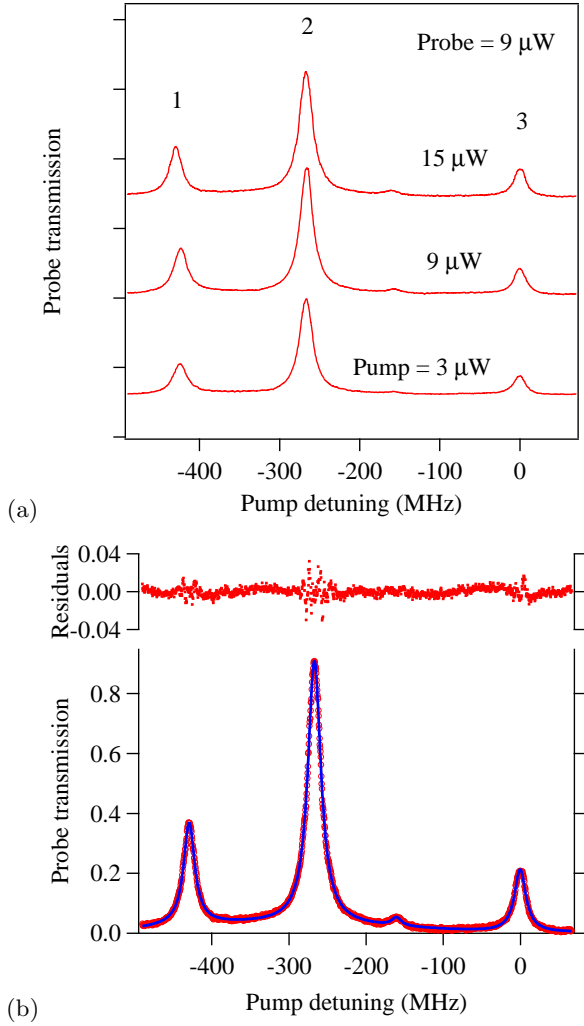


FIG. 4: (a) Spectra taken with co-propagating pump-probe beams at three values of pump power. The probe beam is locked to the $F = 2 \rightarrow 3$ transition and the pump beam is scanning. (b) Spectrum taken at the pump power of $15 \mu\text{W}$ shown with a multipeak Lorentzian fit. The fit residuals are on top.

B. Spectrum in ^{87}Rb , $F = 1 \rightarrow F' = 0, 1, 2$

The same advantages are seen in the spectrum of transitions starting from the lower ground hyperfine level ($F = 1 \rightarrow F' = 0, 1, 2$) shown in Fig. 5. The Doppler-subtracted saturated-absorption spectrum on top has 6 peaks including the 3 crossover resonances. The spectrum with the co-propagating beams shown below is taken with the probe locked to the $F = 1 \rightarrow 0$ transition. The beam powers are $9 \mu\text{W}$ (probe) and $15 \mu\text{W}$ (pump). It appears on a flat background and shows the 3 hyperfine peaks without any crossovers in between. The 3 hyperfine peaks are located at 0, $+72.223 \text{ MHz}$, and $+229.166 \text{ MHz}$. Two of the additional peaks are seen, one at -72.223 MHz (outside the spectrum) and the

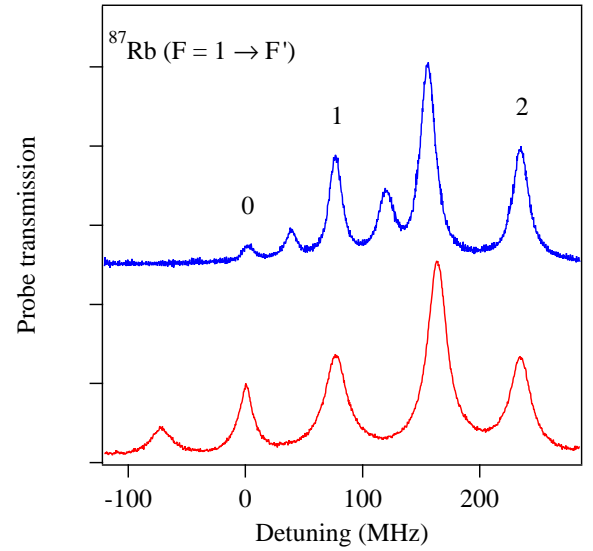


FIG. 5: Comparison of spectra with the two techniques for lower-level $F = 1 \rightarrow F'$ transitions in ^{87}Rb . The upper trace is the Doppler-subtracted saturated-absorption spectrum, while the lower trace is obtained with the probe locked to the $F = 1 \rightarrow 0$ transition and pump scanning.

other at $+156.943 \text{ MHz}$ (within the spectrum). The additional peak within the spectrum is due to atoms moving with a velocity of 52 m/s such that the probe drives the $F = 1 \rightarrow F' = 1$ transition and the pump drives the $F = 1 \rightarrow F' = 2$ transition. This spurious peak is more prominent compared to transitions starting from the upper ground level [see Fig. 2(b)] (though the real peaks still have high signal-to-noise ratio). The difference arises due to the fact that the closed transition for this set is the $F = 1 \rightarrow F' = 0$ transition, which has fewer magnetic sublevels in the excited state compared to the ground state. This leads to population trapping in the $m_F = \pm 1$ sublevels, and the relative importance of EIT effects in causing probe transparency (which is the same for all peaks) increases.

C. Spectrum in ^{85}Rb , $F = 3 \rightarrow F' = 2, 3, 4$

The improvement with this technique is much more dramatic in the spectra of the other isotope, ^{85}Rb . For transitions starting from the upper ground level ($F = 3 \rightarrow F' = 2, 3, 4$) shown in Fig. 6, the hyperfine peaks corresponding to $F' = 2$ and 4 in the saturated-absorption spectrum are barely visible. In the co-propagating spectrum shown below, the peaks become prominent. The hyperfine intervals [10] are such that the real peaks are at -184.390 MHz , -120.966 MHz , and 0 , while the additional peaks are at -63.424 MHz , $+63.424 \text{ MHz}$, $+120.966 \text{ MHz}$, and $+184.390 \text{ MHz}$. The additional peak within the spectrum (at -63.424 MHz) is almost negligible, as was observed for upper-level transitions in ^{87}Rb .

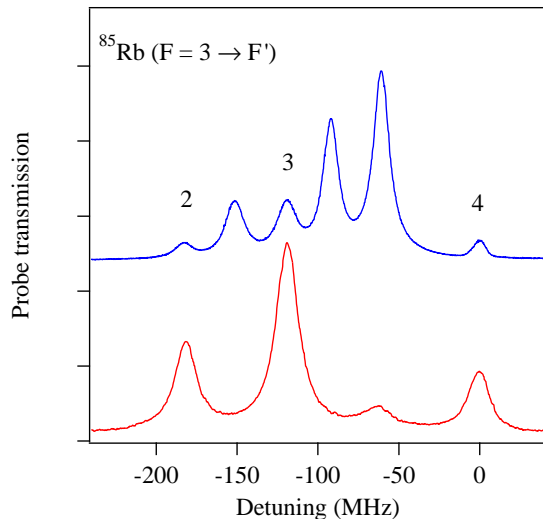


FIG. 6: Comparison of spectra with the two techniques for upper-level $F = 3 \rightarrow F'$ transitions in ^{85}Rb . The upper trace is the Doppler-subtracted saturated-absorption spectrum, while the lower trace is obtained with the probe locked to the $F = 3 \rightarrow 4$ transition and pump scanning.

The beam powers are $9 \mu\text{W}$ (probe) and $15 \mu\text{W}$ (pump).

D. Spectrum in ^{85}Rb , $F = 2 \rightarrow F' = 1, 2, 3$

For transitions starting from the lower ground level ($F = 2 \rightarrow F' = 1, 2, 3$) shown in Fig. 7, the hyperfine interval between $F' = 1$ and 2 is so small that the crossover resonance in the saturated-absorption spectrum completely swamps the $F' = 1$ peak. However, the spectrum with the co-propagating technique shows the peak well resolved. The real peaks are located at 0 , $+29.268$ MHz, and $+92.692$ MHz, while the additional peaks are at -92.692 MHz, -63.424 MHz, -29.268 MHz, and $+63.424$ MHz [10]. The additional peak within the spectrum (at $+63.424$ MHz) is quite prominent as in the case of transitions starting from the lower hyperfine level in ^{87}Rb , again because the closed $F = 2 \rightarrow F' = 1$ transition has population trapping in the $m_F = \pm 2$ sub-levels. There are two additional peaks appearing outside the spectrum to the left, which are closer because of the smaller hyperfine intervals. The beam powers are $9 \mu\text{W}$ (probe) and $15 \mu\text{W}$ (pump).

III. HYPERFINE MEASUREMENTS USING AN ACOUSTO-OPTIC MODULATOR

The above experiments were done using separate pump and probe lasers. However, it is possible to do the experiment with just one laser by using an AOM to produce the scanning pump beam. The scan range of an AOM is limited to about 20 MHz, but this is large enough to

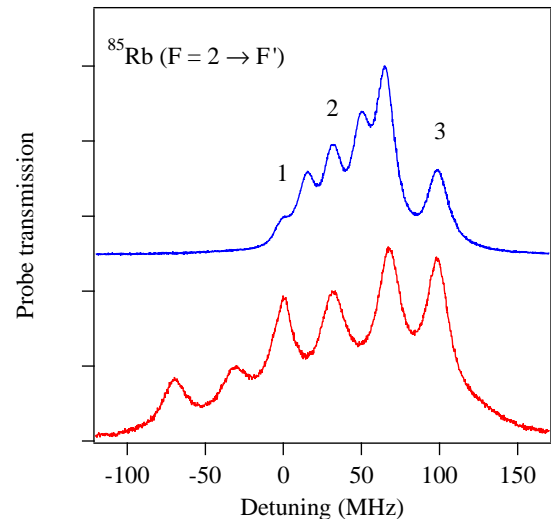


FIG. 7: Comparison of spectra with the two techniques for lower-level $F = 2 \rightarrow F'$ transitions in ^{85}Rb . The upper trace is the Doppler-subtracted saturated-absorption spectrum, while the lower trace is obtained with the probe locked to the $F = 2 \rightarrow 1$ transition and pump scanning.

scan across a hyperfine peak. The main advantage of using an AOM is that the frequency-scan axis (with respect to the probe beam) is both linear and calibrated by the rf frequency of the driver powering the AOM, thus allowing the hyperfine interval to be measured accurately. By measuring the entire peak, potential systematic errors due to locking of the pump laser to a peak are avoided. In addition, if there is a systematic shift in the lock point of the probe laser, this will not cause an error in the interval because the frequency which brings the pump into resonance will also be shifted by the same amount, and hence the AOM offset (with respect to the probe) for the spectrum will remain the same.

We have therefore used a single laser and a scanning AOM to measure hyperfine intervals in the D_2 lines of Rb and Cs. The measurements are motivated by the fact that there are several experimental values reported in the literature that are somewhat discrepant from each other. In many cases, we feel that a potential source of error is the uncertainty in locking to a peak. In our current technique, measuring the entire spectrum avoids such errors, as discussed before.

The experimental schematic for this second set of experiments is shown in Fig. 8. As before, the primary laser is a frequency-stabilized diode laser. The probe beam is derived after locking the laser to a hyperfine transition using SAS. The scanning pump beam is frequency offset from the probe using a double-passed AOM. The frequency is adjusted so that the pump is resonant with a nearby hyperfine transition whose interval has to be measured. The pump intensity is stabilized to better than 1% in a servo-loop by controlling the rf power driving the AOM. The two beams co-propagate through a vapor cell

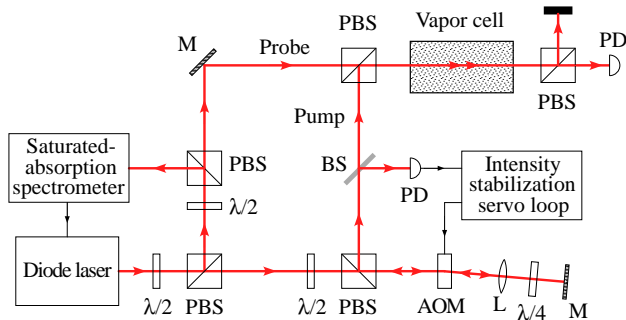


FIG. 8: Schematic of the experiment. Figure key: $\lambda/2$ – halfwave retardation plate, PBS – polarizing beamsplitter cube, AOM – acousto-optic modulator, L – lens, $\lambda/4$ – quarterwave retardation plate, M – mirror, BS – beam splitter, PD – photodiode.

kept inside a magnetic shield. The residual field (measured with a three-axis fluxgate magnetometer) is below 5 mG. The beams have orthogonal linear polarizations and are mixed and separated using PBS's. The beam powers are about $15 \mu\text{W}$ each and adjusted to get good signal-to-noise ratio in the spectrum.

The experiment proceeds as follows. An rf frequency generator whose timebase is referenced to an ovenized quartz clock (uncertainty less than 10^{-8}) is used to drive the AOM. A computer program is used to set the rf frequency, and the probe signal is measured and recorded. The frequency is changed in steps of 0.1 MHz over a range of 15 MHz to obtain the complete spectrum. A curve fit to the spectrum yields the AOM frequency at the peak center, which is the hyperfine interval.

A. Error analysis

Systematic errors can arise due to one of the following reasons.

- (i) *Radiation-pressure effects.* Radiation pressure causes velocity redistribution of the atoms in the vapor cell. In the SAS technique, the opposite Doppler shifts for the counter-propagating beams can result in asymmetry of the observed lineshape. However, with co-propagating beams, the effects are less important because the Doppler shift will be the same for both beams and will not affect the hyperfine interval, similar to how the interval is insensitive to any detuning of the probe from resonance.
- (ii) *Effect of stray magnetic fields.* The primary effect of a magnetic field is to split the Zeeman sublevels and broaden the line without affecting the line center. However, line shifts can occur if there is asymmetric optical pumping into Zeeman sublevels. For a transition $|F, m_F\rangle \rightarrow |F', m_{F'}\rangle$, the systematic shift of the line center is $\mu_B(g_{F'}m_{F'} - g_F m_F)B$,

where $\mu_B = 1.4 \text{ MHz/G}$ is the Bohr magneton, g 's denote the Landé g factors of the two levels, and B is the magnetic field. The selection rule for dipole transitions is $\Delta m = 0, \pm 1$, depending on the direction of the magnetic field and the polarization of the light. Thus, if the beams are linearly polarized, there will be no asymmetric driving and the line center will not be shifted. We therefore minimize this error in two ways. First, we use polarizing cubes to ensure that the beams have near-perfect linear polarization. Second, we use a magnetic shield around the cell to minimize the field.

The experiment is repeated by reversing the scan direction to check for errors that might depend on which direction the rf generator is scanned. Another source of error is whether the intensity stabilization servo-loop stays locked. But if this loses lock, it shows up in the spectrum as an asymmetry of the line shape. Indeed, both the sources of error discussed above also show up as asymmetry of the line shape. Thus a symmetric line shape is a good indication that the measurement proceeded correctly. From the residual asymmetry, we estimate the systematic errors to be 20 kHz.

B. Measurements in the $5P_{3/2}$ state of ^{87}Rb

The first set of measurements were done in ^{87}Rb . The different values in the literature are consistent with each other, and have an accuracy of 10 kHz. Therefore, our main motivation was to see if the scanning-AOM technique worked well and our error budget was proper.

A typical spectrum with the probe locked to the $F = 2 \rightarrow F' = 3$ transition and pump scanning across the $F = 2 \rightarrow F' = 2$ transition is shown in Fig. 9. We saw earlier that the line shape was well described by a Lorentzian. We therefore fit a Lorentzian curve to the spectrum and extract the peak center. Note the symmetry of the spectrum and the high signal-to-noise ratio. The $\{3-2\}$ interval is twice the center frequency (because the AOM is double passed). For technical reasons, there is an additional AOM with a fixed frequency in the path of the probe, and this offset has to be added to obtain the interval.

The average value from 14 individual measurements is listed in Table I. The standard deviation of the set is 32 kHz, which means the expected error in the mean is $32/\sqrt{14} = 8.6 \text{ kHz}$, less than our estimated error of 20 kHz. This value is compared to other values reported in the literature. The two most accurate measurements [10, 13] have uncertainties below 10 kHz and have overlapping error bars. The more recent measurement [10] is also from our laboratory and used an AOM to measure the interval, but the AOM was locked to the peak. The current measurement obtained by measuring the entire spectrum is consistent with this value, thus giving confidence in the current technique. The only slightly

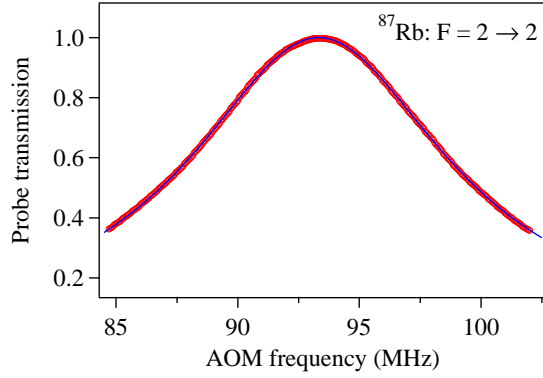


FIG. 9: Spectrum in ^{87}Rb with probe locked to the $F = 2 \rightarrow 3$ transition, and pump scanning across the $F = 2 \rightarrow 2$ transition. The solid curve is a fit to a Lorentzian lineshape.

TABLE I: Comparison of measurements of hyperfine intervals in the $5P_{3/2}$ state of ^{87}Rb to previous results. The last row is calculated from the A and B coefficients reported therein. All values in MHz.

$\{3 - 2\}$ Interval	Reference
266.653(20)	This work
266.657(8)	[10]
266.650(9)	[13]
266.503(84)	[14]

discrepant measurement is from the work in Ref. [14], which is 1.7σ away.

C. Measurements in the $5P_{3/2}$ state of ^{85}Rb

With the reliability of the technique established with measurements in ^{87}Rb , we turned to the other isotope, namely ^{85}Rb . The probe was locked to the $F = 3 \rightarrow F' = 4$ transition, and the pump was scanned either across the $F = 3 \rightarrow F' = 3$ transition or the $F = 3 \rightarrow F' = 2$ transition. Typical spectra for the two cases are shown in Fig. 10. As before, Lorentzian fits to the measured spectra were used to determine the peak center, and thus the $\{4 - 3\}$ and $\{3 - 2\}$ intervals.

The average values for the two intervals are listed in Table II. For the $\{4 - 3\}$ interval, the standard deviation from a set of 14 measurements is 35 kHz. For the $\{3 - 2\}$ interval, the standard deviation from 11 measurements is 34 kHz. These values are also compared to other values in the literature. There are two non-overlapping sets for the $\{4 - 3\}$ interval. The value from Ref. [14] is 3.7σ away from the other two values, which are both from our laboratory and both of which relied on AOM locking. Ref. [14] is also the work in which the value in ^{87}Rb was discrepant by 1.7σ . The current measurement is consistent with our previous ones. All the values for the $\{3 - 2\}$ interval are consistent with each other.

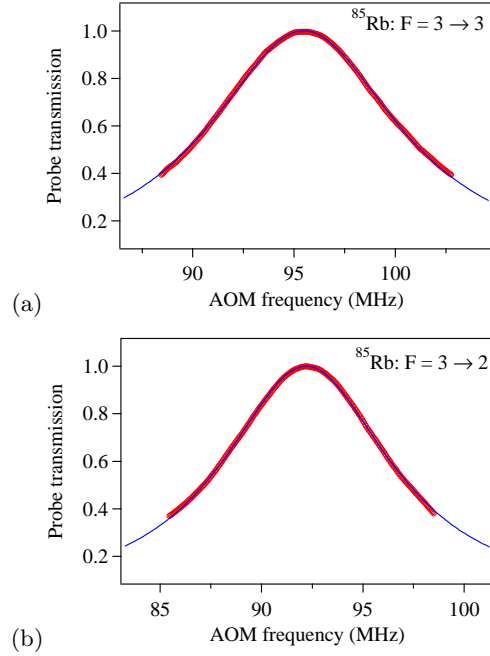


FIG. 10: Spectra in ^{85}Rb with probe beam locked to the $F = 3 \rightarrow 4$ transition, and pump beam scanning across (a) the $F = 3 \rightarrow 3$ transition, and (b) the $F = 3 \rightarrow 2$ transition. The solid curves are Lorentzian fits.

TABLE II: Comparison of measurements of hyperfine intervals in the $5P_{3/2}$ state of ^{85}Rb to previous results. The last row is calculated from the A and B coefficients reported therein. All values in MHz.

$\{4 - 3\}$ Interval	$\{3 - 2\}$ Interval	Reference
120.958(20)	63.436(20)	This work
120.966(8)	63.424(6)	[10]
120.960(20)	63.420(31)	[15]
120.506(124)	63.402(93)	[14]

D. Measurements in the $6P_{3/2}$ state of ^{133}Cs

The next set of measurements was done on the D_2 line in ^{133}Cs at 852 nm. For this, the probe was locked to the $F = 4 \rightarrow F' = 5$ transition and the pump was scanned either across the $F = 4 \rightarrow F' = 4$ transition or the $F = 4 \rightarrow F' = 3$ transition. Representative spectra for the two cases are shown in Fig. 11. Lorentzian fits to the spectra yielded the line center and hence the $\{5 - 4\}$ and $\{4 - 3\}$ intervals.

The average value for the $\{5 - 4\}$ interval is 251.031(20) MHz, as listed in Table III. This was obtained from a set of 27 independent measurements with a standard deviation of 21 kHz. We concentrated on this interval because two of the values reported in the literature, 251.092(2) MHz from Ref. [16] and 251.000(20) from Ref. [17], differ by 4.5σ . The more recent measurement of the two [16] was done using a frequency comb. An earlier measurement from our laboratory using the AOM locking

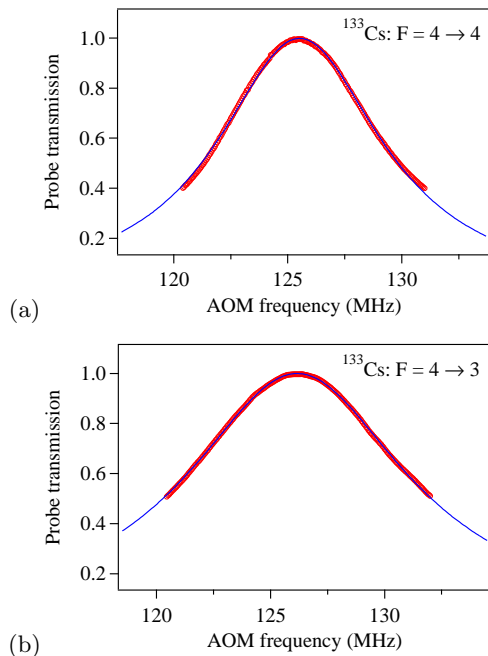


FIG. 11: Spectra in ^{133}Cs with probe beam locked to the $F = 4 \rightarrow 5$ transition, and pump beam scanning across (a) the $F = 4 \rightarrow 4$ transition, and (b) the $F = 4 \rightarrow 3$ transition. The solid curve are Lorentzian fits.

TABLE III: Comparison of measurements of hyperfine intervals in the $6P_{3/2}$ state of ^{133}Cs to previous results. All values in MHz.

{5 – 4} Interval	{4 – 3} Interval	Reference
251.031(20)	201.260(20)	This work
251.037(6)	201.266(6)	[9]
251.092(2)	201.287(1)	[16]
251.000(20)	201.240(20)	[17]

technique [9] yielded a result of 251.037(6) MHz, which was consistent with the earlier value at the 1.5σ level, but totally inconsistent with the frequency-comb result (difference of 9σ). Our current value vindicates our earlier result since it is consistent with the work in Ref. [17] but not with the frequency-comb result.

For the {4 – 3} interval, we obtain an average value of 201.260(20) MHz from a set of 10 measurements with a standard deviation of 33 kHz. The value from the work in Ref. [17] was 201.240(20) MHz, while the more recent frequency-comb work in Ref. [16] reported a value of 201.287(1) MHz. The inconsistency of 2.4σ is smaller but still quite significant. Again, our previous result of

201.266(6) MHz obtained with AOM locking [9] overlapped with the earlier value but was inconsistent with the frequency-comb result. Our new value, though with a larger error bar, gives confidence in the previous measurement.

IV. CONCLUSIONS

In summary, we have shown that hyperfine spectroscopy with co-propagating beams in a vapor cell has several advantages over conventional saturated-absorption spectroscopy. In addition to the usual mechanisms responsible for probe transparency, there are EIT effects that enhance the peaks, which is supported by density-matrix calculations. As a result, the primary peaks are more prominent and appear with good signal-to-noise ratio. The transmitted signal appears on a flat background (Doppler-free) and does not have the problem of crossover resonances in between hyperfine transitions (which are stronger and often swamp the true peaks). Absorption by non-zero velocity groups causes additional peaks, but only one of them appears within the spectrum. These observations are again supported by density-matrix calculations taking the thermal velocity distribution into account. An important difference between transitions starting from the upper ground level and transitions starting from the lower ground level, is that the additional peak is almost negligible in the first case and quite prominent in the second case. This difference arises because of the difference in number of magnetic sublevels for the closed transition in each set.

We have adapted this technique to make measurements of hyperfine intervals by using one laser along with an AOM to produce the scanning pump beam. We measure intervals in the D_2 lines of Rb and Cs with 20 kHz precision. By measuring the entire spectrum and looking at the symmetry of the line shape, we avoid several potential sources of systematic error. The measurements are consistent with earlier results from our laboratory obtained by locking the AOM to the frequency difference, and show that our earlier error budget was reasonable.

Acknowledgments

This work was supported by the Department of Science and Technology, India. V.N. acknowledges support from the Homi Bhabha Fellowship Council and A.K.S. from the Council of Scientific and Industrial Research, India.

-
- [1] C. E. Wieman and L. Hollberg, “Using diode lasers for atomic physics,” *Rev. Sci. Instrum.* **62**, 1–20 (1991).
 - [2] K. B. MacAdam, A. Steinbach, and C. Wieman, “A narrow-band tunable diode laser system with grating

- feedback, and a saturated absorption spectrometer for Cs and Rb,” *Am. J. Phys.* **60**, 1098–1111 (1992).
- [3] A. Banerjee, U. D. Rapol, A. Wasan, and V. Natarajan, “High-accuracy wavemeter based on a stabilized diode

- laser,” *Appl. Phys. Lett.* **79**, 2139–2141 (2001).
- [4] M. S. Safronova, W. R. Johnson, and A. Derevianko, “Relativistic many-body calculations of energy levels, hyperfine constants, electric-dipole matrix elements, and static polarizabilities for alkali-metal atoms,” *Phys. Rev. A* **60**, 4476–4487 (1999).
 - [5] E. Arimondo, M. Inguscio, and P. Violino, “Experimental determinations of the hyperfine structures in the alkali atoms,” *Rev. Mod. Phys.* **49**, 31–75 (1977).
 - [6] W. Demtröder, *Laser Spectroscopy* (Springer-Verlag, Berlin, 2003), 3rd ed.
 - [7] A. Banerjee and V. Natarajan, “Saturated-absorption spectroscopy: eliminating crossover resonances by use of copropagating beams,” *Opt. Lett.* **28**, 1912–14 (2003).
 - [8] S. E. Harris, “Electromagnetically induced transparency,” *Phys. Today* **50**, 36–39 (1997).
 - [9] D. Das and V. Natarajan, “Hyperfine spectroscopy on the $6P_{3/2}$ state of ^{133}Cs using coherent control,” *Europhys. Lett.* **72**, 740–746 (2005).
 - [10] D. Das and V. Natarajan, “High-precision measurement of hyperfine structure in the D lines of alkali atoms,” *J. Phys. B* **41**, 035001 (12pp) (2008).
 - [11] C. Cohen-Tannoudji and S. Reynaud, “Modification of resonance Raman scattering in very intense laser fields,” *J. Phys. B* **10**, 365–383 (1977).
 - [12] P. R. S. Carvalho, L. E. E. de Araujo, and J. W. R. Tabosa, “Angular dependence of an electromagnetically induced transparency resonance in a Doppler-broadened atomic vapor,” *Phys. Rev. A* **70**, 063818 (2004).
 - [13] J. Ye, S. Swartz, P. Jungner, and J. L. Hall, “Hyperfine structure and absolute frequency of the ^{87}Rb $5P_{3/2}$ state,” *Opt. Lett.* **21**, 1280–1282 (1996).
 - [14] G. P. Barwood, P. Gill, and W. R. C. Rowley, “Frequency measurements on optically narrowed Rb-stabilised laser diodes at 780 nm and 795 nm,” *Appl. Phys. B* **53**, 142–147 (1991).
 - [15] U. D. Rapol, A. Krishna, and V. Natarajan, “Precise measurement of the hyperfine structure in the $5P_{3/2}$ state of ^{85}Rb ,” *Eur. Phys. J. D* **23**, 185–188 (2003).
 - [16] V. Gerginov, A. Derevianko, and C. E. Tanner, “Observation of the nuclear magnetic octupole moment of ^{133}Cs ,” *Phys. Rev. Lett.* **91**, 072501 (2003).
 - [17] C. E. Tanner and C. Wieman, “Precision measurement of the hyperfine structure of the ^{133}Cs $6P_{3/2}$ state,” *Phys. Rev. A* **38**, 1616–1617 (1988).